

## Universal Formula for the Mean First Passage Time in Planar Domains

Denis S. Grebenkov\*

Laboratoire de Physique de la Matière Condensée (UMR 7643), CNRS—Ecole Polytechnique, University Paris-Saclay,  
91128 Palaiseau, France

(Received 20 September 2016; revised manuscript received 13 November 2016; published 23 December 2016)

We derive a general exact formula for the mean first passage time (MFPT) from a fixed point inside a planar domain to an escape region on its boundary. The underlying mixed Dirichlet-Neumann boundary value problem is conformally mapped onto the unit disk, solved exactly, and mapped back. The resulting formula for the MFPT is valid for an arbitrary space-dependent diffusion coefficient, while the leading logarithmic term is explicit, simple, and remarkably universal. In contrast to earlier works, we show that the natural small parameter of the problem is the harmonic measure of the escape region, not its perimeter. The conventional scaling of the MFPT with the area of the domain is altered when diffusing particles are released near the escape region. These findings change the current view of escape problems and related chemical or biochemical kinetics in complex, multiscale, porous or fractal domains, while the fundamental relation to the harmonic measure opens new ways of computing and interpreting MFPTs.

DOI: 10.1103/PhysRevLett.117.260201

How long does it take for diffusing species to exit from an irregular domain or to initiate a reaction on a catalytic site or an enzyme? Since the first contribution by Lord Rayleigh [1], the first-passage phenomena have attracted much attention [2–5], and have been applied to numerous chemical [6] and biological [7] problems such as diffusion-influenced ligand binding to receptors on cell surfaces [8,9], receptor trafficking in synaptic membranes [10], diffusion in cellular microdomains [11], or foraging strategies of animals [12], to name but a few. Most analytical results were obtained for the mean first passage time (MFPT) to a small region on the boundary, which can represent a specific target, a catalytic germ, an active site, a channel, or an exit to the outer space [5,13–21]. For a “regular” planar domain  $\Omega$  (whose perimeter  $|\partial\Omega|$  and linear size  $|\Omega|^{1/2}$  are comparable, see Ref. [5]), the MFPT, averaged over uniformly distributed starting points, was shown to be  $|\Omega|/(\pi D)[\ln(1/\varepsilon) + O(1)]$ , where  $D$  is the diffusion coefficient,  $|\Omega|$  is the area of the domain, and  $\varepsilon = |\Gamma|/|\partial\Omega| \ll 1$  is the perimeter of the escape region  $\Gamma$  divided by the perimeter of the boundary  $\partial\Omega$  [14]. In the special case of a disk, Singer *et al.* also showed that the MFPT from a fixed starting point (e.g., the center) exhibits similar  $\ln(1/\varepsilon)$  behavior [15]. Since these seminal works, the logarithmic divergence of the MFPT with respect to the normalized perimeter  $\varepsilon$  has become a common paradigm (see the review in Ref. [5] and references therein).

In this Letter, we show that this paradigm is incomplete for general domains and can be strongly misleading when the starting point is fixed. We derive the exact formula for the MFPT from a fixed point  $x_0$  to a connected escape region  $\Gamma$  on the boundary of any simply connected (i.e., without “holes”) planar domain  $\Omega$ . This formula is not restricted to the narrow escape limit  $\varepsilon \ll 1$  and is valid for

an arbitrary space-dependent diffusion coefficient. Most importantly, we reveal an earlier unnoticed fundamental relation between the MFPT and the harmonic measure of the escape region,  $\omega = \omega_{x_0}(\Gamma)$ , i.e., the probability of arriving at the escape region  $\Gamma$  before hitting the remaining part of the boundary [22].

Before proceeding to rigorous results, we start with two examples of “nonregular” domains casting doubts on the normalized perimeter  $\varepsilon$  as the universal small parameter. If the domain is a thin long rectangle  $[0, L] \times [0, h]$ , the MFPT to the left short edge from a starting point  $x_0 = (x_0^1, x_0^2)$  is equal to  $(Lx_0^1 - \frac{1}{2}[x_0^1]^2)/D$ . Being independent of  $h$ , this MFPT is thus not determined by the normalized perimeter  $\varepsilon = \frac{1}{2}h/(L+h)$ , even if the latter is very small. In the second example, one takes a disk and replaces a small arc of its boundary by a very corrugated (e.g., fractal) curve. Keeping the diameter  $\delta$  of the modified escape region small, one can make its perimeter arbitrarily large. Since the remaining part of the circle is fixed, the ratio  $\varepsilon = |\Gamma|/|\partial\Omega|$  can be made close to 1. When  $\delta$  is small, the MFPT should be large, in spite the fact of  $\varepsilon \approx 1$ . These two very basic examples illustrate the failure of the normalized perimeter of the escape region as a determinant of the MFPT when the starting point is fixed. We will show that the natural characteristic that substitutes the normalized perimeter  $\varepsilon$  is the harmonic measure  $\omega_{x_0}(\Gamma)$ .

For Brownian motion starting from an interior point  $x_0$  of a simply connected planar domain  $\Omega$ , the MFPT  $T(x_0)$  to a connected escape region  $\Gamma$  on the boundary  $\partial\Omega$  satisfies the backward Fokker-Planck equation [23]

$$\Delta T(x_0) = -\frac{1}{D(x_0)}, \quad x_0 \in \Omega \quad (1)$$

with mixed Dirichlet-Neumann boundary conditions

$$\begin{aligned} \mathcal{T}(x_0) &= 0, & x_0 \in \Gamma, \\ \partial_n \mathcal{T}(x_0) &= 0, & x_0 \in \partial\Omega \setminus \Gamma, \end{aligned} \quad (2)$$

where  $\partial_n$  is the normal derivative,  $\Delta$  is the Laplace operator, and  $D(x_0)$  is the space-dependent diffusion coefficient. According to the Riemann mapping theorem, the unit disk  $\mathcal{D}$  can be mapped onto  $\Omega$  by a conformal mapping  $\phi_{x_0}(z): \mathcal{D} \rightarrow \Omega$ . We fix two parameters of the conformal map by imposing that the origin of  $\mathcal{D}$  is mapped onto the starting point  $x_0$ :  $\phi_{x_0}(0) = x_0$ . Since the conformal mapping preserves the harmonic measure, the preimage of  $\Gamma$  is an arc  $\gamma$  of the unit circle of length  $2\pi\omega$ . Note that the harmonic measure is fully determined by the conformal map. The third parameter of the conformal mapping is fixed by rotating the arc  $\gamma$  to be  $(-\pi\omega, \pi\omega)$ . Setting  $\tau(z) = \mathcal{T}(\phi_{x_0}(z))$  for  $z \in \mathcal{D}$ , Eqs. (1) and (2) are transformed into

$$\begin{aligned} \Delta \tau(z) &= -|\phi'_{x_0}(z)|^2/D(\phi_{x_0}(z)), & z \in \mathcal{D}, \\ \tau(z) &= 0, & z \in \gamma, \\ \partial_n \tau(z) &= 0, & z \in \partial\mathcal{D} \setminus \gamma. \end{aligned} \quad (3)$$

The solution of this mixed boundary value problem can be reduced to dual trigonometric equations whose solutions are well documented [24]. Skipping mathematical details (see Sec. I of the Supplemental Material [25]), we obtain for any interior starting point  $x_0 \in \Omega$

$$\mathcal{T}(x_0) = \int_{\mathcal{D}} \frac{dz |\phi'_{x_0}(z)|^2}{D(\phi_{x_0}(z))} \left( -\frac{\ln|z|}{2\pi} + W_\omega(z) \right) \quad (4)$$

with

$$W_\omega(z) = \frac{1}{\pi} \ln \left( \frac{|1-z + \sqrt{(1-ze^{i\pi\omega})(1-ze^{-i\pi\omega})}|}{2 \sin(\pi\omega/2)} \right), \quad (5)$$

in which the most challenging “ingredient” of the problem, the mixed boundary condition, is fully incorporated through the explicit function  $W_\omega(z)$ . The function  $W_\omega(z)$  is universal; its dependence on  $\Omega$ ,  $\Gamma$ , and  $x_0$  enters uniquely through the harmonic measure  $\omega = \omega_{x_0}(\Gamma)$ . To return to the domain  $\Omega$ , the integration variable  $z$  is changed to  $x = \phi_{x_0}(z)$ , which yields

$$\mathcal{T}(x_0) = \int_{\Omega} \frac{dx}{D(x)} \underbrace{\left( -\frac{\ln|\phi_{x_0}^{-1}(x)|}{2\pi} + W_{\omega_{x_0}}(\phi_{x_0}^{-1}(x)) \right)}_{\text{Green's function}}. \quad (6)$$

The exact solution (6) is our main result. The two terms are, respectively, (i) the MFPT from  $x_0$  to the whole boundary  $\partial\Omega$ , with  $(2\pi)^{-1} \ln|\phi_{x_0}^{-1}(x)|$  being the Dirichlet

Green’s function in  $\Omega$ , and (ii) the contribution from eventual reflections on the remaining part of the boundary,  $\partial\Omega \setminus \Gamma$ , until reaching the escape region  $\Gamma$ . The integral form of the solution  $\mathcal{T}(x_0)$ , which is valid for an arbitrary function  $1/D(x)$ , allows one to interpret the expression in parentheses in Eq. (6) as the Green’s function of the Laplace operator  $-\Delta$  subject to mixed Dirichlet-Neumann boundary condition (2). Numerical implementation of the exact solution (6), its accuracy, and a comparison to conventional numerical methods for computing MFPTs are discussed in Sec. II of the Supplemental Material [25]. While conformal mappings have been intensively used to solve diffusion-reaction problems (e.g., see Refs. [5,27–36] and references therein), this powerful technique is applied to the mixed boundary value problem in Eqs. (1) and (2) for the first time. Prior to this work, no exact solution of this MFPT problem was available, except for a few simple domains [15,20,21]. While the proposed approach is limited to planar Brownian diffusion (see the further discussion in Sec. I of the Supplemental Material [25]), the universality of the exact solution (6) results from the existence of a conformal map for any simply connected planar domain, even with a very irregular (e.g., fractal) boundary. The only mathematical restriction on the domain is that the original problem in Eqs. (1) and (2) should be well defined. In the case of the unit disk with a constant diffusivity, our general formula (6) reduces to the earlier result [20]

$$\mathcal{T}(x_0) = \frac{1 - |x_0|^2}{4D} + \frac{\pi}{D} W_\varepsilon(x_0) \quad (7)$$

(see Sec. III of the Supplemental Material [25] for the derivation).

The general solution (6) allows one to investigate, for the first time, the impact of heterogeneous diffusivity in MFPT problems defined in nontrivial domains. In spite of its evident importance for biological systems in which the spatial heterogeneity is ubiquitous, only a few analytical results about one-dimensional motion with space-dependent diffusivity are available (e.g., see Ref. [37]). Even for simple domains such as disks or rectangles, the spatial dependence of the diffusion coefficient can prohibit the separation of variables or, in the most favorable cases, lead to complicated differential equations whose solutions cannot be expressed in terms of usual special functions. In this light, it is remarkable that the formula (6) provides an exact solution even for the space-dependent diffusivity  $D(x)$ . One can investigate, e.g., how the lower diffusivity in the actin cortex near the plasma membrane would affect the overall MFPT in flat living cells adhered to a surface, as well as the effect of corrals on membrane diffusion.

When the harmonic measure of the escape region is small, one can derive the perturbative expansion of the MFPT (see Sec. IV of the Supplemental Material [25]):

$$\begin{aligned} \mathcal{T}(x_0) = & \frac{|\Omega|}{\pi D_h} \ln(1/\omega) \\ & + \left( \frac{|\Omega| \ln(2/\pi)}{\pi D_h} + \frac{1}{2\pi} \int_{\Omega} \frac{dx}{D(x)} \ln \frac{|1 - \phi_{x_0}^{-1}(x)|^2}{|\phi_{x_0}^{-1}(x)|} \right) \\ & + \omega^2 \left( \frac{\pi |\Omega|}{24 D_h} - \int_{\Omega} dx \frac{V_2(\phi_{x_0}^{-1}(x))}{D(x)} \right) + O(\omega^4) \end{aligned} \quad (8)$$

with

$$V_2(z) = -\frac{\pi}{8} \left( \frac{z}{(1-z)^2} + \frac{\bar{z}}{(1-\bar{z})^2} \right). \quad (9)$$

The first logarithmic term appears as the leading contribution that involves the harmonic measure of the escape region,  $\omega = \omega_{x_0}(\Gamma)$ , the area of the domain,  $|\Omega|$ , and the harmonic mean of the space-dependent diffusion coefficient:

$$\frac{1}{D_h} = \frac{1}{|\Omega|} \int_{\Omega} \frac{dx}{D(x)} \quad (10)$$

[if  $D(x) = D$  is constant, then  $D_h = D$ ]. The expansion (8) and its leading term  $|\Omega|/(\pi D_h) \ln(1/\omega_{x_0})$  present the second main result that allows one to estimate the MFPT directly through the harmonic measure.

In fact, when the starting point  $x_0$  is not too close to the boundary, the leading term provides a good approximation to the MFPT. To illustrate this point, we generated a planar domain in Fig. 1(a) by iterative conformal maps (see Sec. V of the Supplemental Material [25]). In order to emphasize that the normalized perimeter  $\varepsilon$  of the escape region must be replaced by the harmonic measure, we fix  $\varepsilon = 0.035$  and then move the escape region  $\Gamma_s$  of perimeter  $\varepsilon|\partial\Omega|$  along the boundary of the domain, where  $s$  is the curvilinear coordinate of the center of  $\Gamma_s$ . Figure 1(b) shows  $\mathcal{T}(x_0)$  from Eq. (6) and its leading term  $-|\Omega|/(\pi D) \ln \omega_{x_0}(\Gamma_s)$  from Eq. (8), as functions of the location  $s$  of the escape region  $\Gamma_s$  on the boundary for  $x_0 = 0$  (we set  $D = 1$  and use dimensionless units). As expected, the MFPT significantly varies when the escape region moves, showing the dependence on the distance between  $x_0$  and  $\Gamma$  and on the shape of the domain. For instance, the corner at the curvilinear location  $s \approx 2.7$  is difficult to access so that the related harmonic measure is very small, while the MFPT exhibits a prominent peak rising up to 14. In turn, three escape regions at  $s \approx 0, 3.7, 7.3$  are the closest to the starting point and thus easily accessible, resulting in the minima of the MFPT. One can see that the leading term with the harmonic measure provides an excellent approximation to the MFPT. In turn, the conventional leading term  $|\Omega|/(\pi D) \ln(1/\varepsilon)$  (which is independent of the location) is a poor estimate, in spite of the fact that  $\varepsilon$  is small. We conclude that when the starting point is fixed, the harmonic measure of the escape region should substitute the

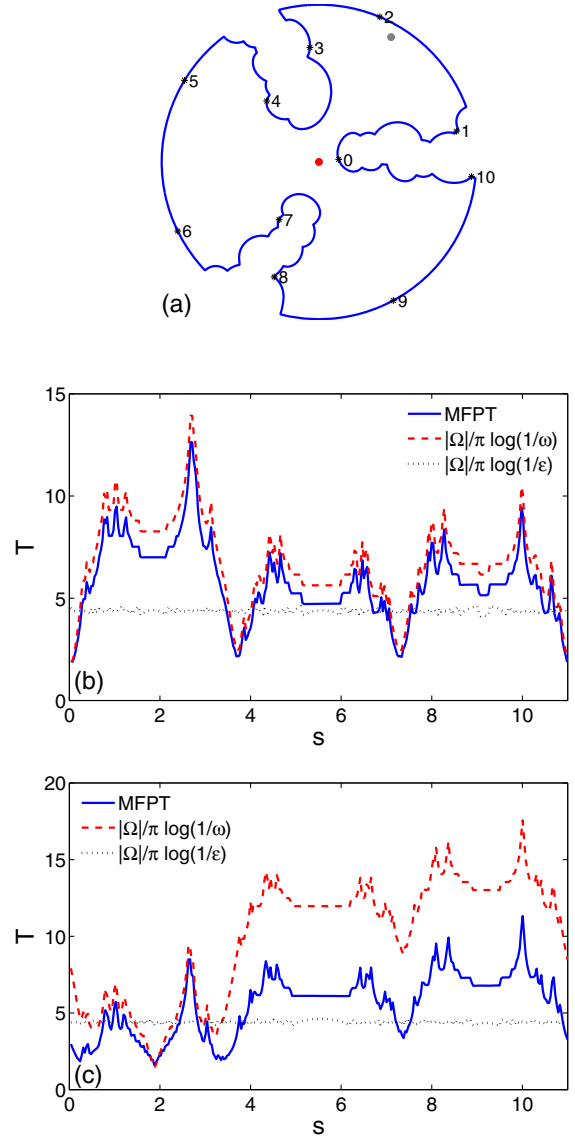


FIG. 1. (a) An irregular domain obtained by iterative conformal maps (see Sec. 5 of the Supplemental Material [25]). The red and gray circles indicate two considered starting points:  $x_0 = 0$  and  $x_0 = 0.4590 + 0.7936i$ ; the asterisks with indicated curvilinear coordinates present “milestones” along the boundary; the perimeter, the diameter, and the area of the domain are 10.96, 2, and 2.39, respectively. (b),(c) The MFPT  $\mathcal{T}(x_0)$  (solid line), the leading term  $|\Omega|/(\pi D) \ln[1/\omega_{x_0}(\Gamma_s)]$  (dashed line), and the conventional leading term  $|\Omega|/(\pi D) \ln(1/\varepsilon)$  (dotted line) as functions of the location  $s$  of the escape region  $\Gamma_s$  on the boundary of the shown domain, with  $x_0 = 0$  (b) and  $x_0 = 0.4590 + 0.7936i$  (c). Note that small fluctuations of the dotted line are related to small variations in the perimeter of the escape region due to discretization. Here, we set  $D = 1$  and use dimensionless units

normalized perimeter as the natural small parameter, at least in two dimensions.

When the starting point  $x_0$  is close to the boundary, the logarithmic term overestimates the MFPT, as illustrated in

Fig. 1(c) for the starting point  $x_0 = 0.4590 + 0.7936i$ . One can see that the logarithmic term accurately captures the behavior of the MFPT when the escape region is close to the starting point ( $s$  between 1 and 3) while a significant but nearly constant deviation appears for distant escape regions. Here, the contribution from the next-order terms in Eq. (8), in particular, that of order  $O(1)$ , is comparable to the logarithmic term.

This situation can also be illustrated on the example of a thin rectangle  $[0, L] \times [0, h]$  that we discussed at the beginning. In fact, the harmonic measure  $\omega$  of the short edge on the left, seen from a point  $(x_0^1, h/2)$ , is approximately  $\exp(-\pi x_0^1/h)$  (see Sec. III of the Supplemental Material [25]). Substitution of this expression into the first term of Eq. (8) yields  $Lx_0^1/D$ , which is close to the exact MFPT  $(Lx_0^1 - \frac{1}{2}[x_0^1]^2)/D$ . This simple example illustrates that (i) even if the harmonic measure  $\omega$  is very small, the contribution from the remaining terms in Eq. (8) can still be significant (e.g., the term  $-\frac{1}{2}[x_0^1]^2/D$  in this example), and (ii) this MFPT does not scale with the area of the domain. Interestingly, even though the area of the rectangle,  $|\Omega| = Lh$ , stands in front of the logarithmic term in Eq. (8), the thickness  $h$  is then removed by the factor  $1/h$  coming from  $\ln \omega$ . The last observation challenges another common paradigm that the MFPT is proportional to the area of the domain. In particular, if particles are released from a fixed point near the escape region, most of them find it very rapidly. Would the contribution to the MFPT from a few particles that miss the escape region at the beginning and thus explore the whole domain ensure the scaling  $\mathcal{T}(x_0) \propto |\Omega|$ ? The answer is in general negative as discussed in Sec. VI of the Supplemental Material [25] and illustrated above in the case of a thin rectangle.

We can now revise the second example mentioned above, namely, a disk with a small but highly corrugated arc. According to Makarov's theorem, the information dimension of the harmonic measure is equal to 1 for planar connected sets [38,39], implying that  $\omega_{x_0}(\Gamma)$  scales with the diameter of  $\Gamma$  [40]. In other words, the harmonic measure of the corrugated arc, seen from a distant point  $x_0$ , is determined by the diameter  $\delta$  of the arc, not the perimeter  $\varepsilon$ . We thus recover the intuitively expected behavior  $|\Omega|/(\pi D) \ln(1/\delta)$  when  $\delta$  is small. In turn, the conventional formula  $|\Omega|/(\pi D) \ln(1/\varepsilon)$  is again strongly misleading. We emphasize that  $\omega$  and  $\varepsilon$  are in general unrelated; e.g., a set may have an arbitrarily small harmonic measure and arbitrarily large perimeter, and vice versa.

These examples illustrate generic features of the MFPT in porous media with long channels or fjords, and in domains with irregular boundaries, in contrast to earlier works that dealt with very regular domains whose perimeter  $|\partial\Omega|$  and linear size  $|\Omega|^{1/2}$  were comparable (see Ref. [5]). In the latter case, the harmonic measure of the escape region is proportional to its Lebesgue measure (i.e., the perimeter), recovering the conventional  $\ln(1/\varepsilon)$

behavior, the proportionality coefficient (the harmonic measure density), and the related dependence on the starting point  $x_0$  being "hidden" in the  $O(1)$  term. We stress that even for such regular domains, the dependence on the starting point can be strong and provide the dominant contribution to the MFPT, as illustrated in Figs. 1(b) and 1(c). For instance, one can think of two pores connected by a very narrow channel. If the particle starts inside one pore while the escape region is located on the boundary of the other pore, the MFPT can be made arbitrarily large by controlling the channel width, even if the escape region remains large whereas the condition  $|\partial\Omega| \sim |\Omega|^{1/2}$  is satisfied. Only the average of  $\mathcal{T}(x_0)$  over the starting point  $x_0$  might recover the  $\ln(1/\varepsilon)$  dependence in the leading term. However, in many applications, the source of particles and the escape region are well separated (e.g., viruses entering the cell at the membrane and searching for the nucleus, or molecules released near the nucleus and searching to escape through the membrane). The proposed formula (6) thus yields a powerful tool to investigate these search and escape phenomena.

The uncovered relation between the MFPT and the harmonic measure brings new opportunities. On one hand, one can profit from numerous analytical and numerical results known for the harmonic measure on irregular boundaries [22,38,39,41–51]. In particular, the concept of diffusion screening [40,52] that has found numerous implications for heterogeneous catalysis [53], fluid flow in rough channels [36,54], and transport phenomena in biological systems [55–58] can now be applied to the MFPT. For instance, the harmonic measure of an escape region at the bottom of a fjord can exhibit various types of decay with the "depth," depending on the shape [22,41]. Similar dependences are thus expected for the MFPT. On the other hand, the conformal mapping is a powerful analytical and numerical technique to represent the geometric complexity of a domain through analytic properties of the mapping function  $\phi_{x_0}(z)$  [59]. The unit disk can be conformally mapped onto any polygon either by a Schwarz-Christoffel formula [60,61] or by a "zipper" algorithm [62]. Once the conformal map is constructed, finding the MFPT in complex domains is reduced to computing the integrals in Eqs. (4) or (6). Most importantly, the proposed approach is not limited to regular domains (with  $|\partial\Omega| \sim |\Omega|^{1/2}$ ) and allows one to study the MFPT for irregular (e.g., fractal) boundaries and branching domains with long rough channels and large surface-to-volume ratios that are relevant for most applications. This approach opens thus a new field of research on first passage times and related chemical or biochemical kinetics in complex, multiscale, and porous media.

The author acknowledges support under Grant No. ANR-13-JSV5-0006-01 of the French National Research Agency, and Dr. A. Rutenberg and Dr. D. Belyaev for fruitful discussions.

- \*denis.grebenkov@polytechnique.edu
- [1] J. W. S. Baron Rayleigh, *The Theory of Sound*, 2nd ed. (Dover, New York, 1945), Vol. 2.
- [2] S. Redner, *A Guide to First Passage Processes* (Cambridge University Press, Cambridge, 2001).
- [3] R. Metzler, G. Oshanin, and S. Redner, *First-Passage Phenomena and Their Applications* (World Scientific, Singapore, 2014).
- [4] O. Bénichou and R. Voituriez, *Phys. Rep.* **539**, 225 (2014).
- [5] D. Holcman and Z. Schuss, *SIAM Rev.* **56**, 213 (2014).
- [6] P. Hänggi, P. Talkner, and M. Borkovec, *Rev. Mod. Phys.* **62**, 251 (1990).
- [7] P. C. Bressloff and J. M. Newby, *Rev. Mod. Phys.* **85**, 135 (2013).
- [8] R. Zwanzig and A. Szabo, *Biophys. J.* **60**, 671 (1991).
- [9] I. V. Grigoriev, Y. A. Makhnovskii, A. M. Berezhkovskii, and V. Y. Zitserman, *J. Chem. Phys.* **116**, 9574 (2002).
- [10] D. Holcman and Z. Schuss, *J. Stat. Phys.* **117**, 975 (2004).
- [11] Z. Schuss, A. Singer, and D. Holcman, *Proc. Natl. Acad. Sci. U.S.A.* **104**, 16098 (2007).
- [12] G. M. Viswanathan, S. V. Buldyrev, S. Havlin, M. G. E. da Luz, E. P. Raposok, and H. E. Stanley, *Nature (London)* **401**, 911 (1999).
- [13] M. J. Ward and J. B. Keller, *SIAM J. Appl. Math.* **53**, 770 (1993).
- [14] A. Singer, Z. Schuss, D. Holcman, and R. S. Eisenberg, *J. Stat. Phys.* **122**, 437 (2006).
- [15] A. Singer, Z. Schuss, and D. Holcman, *J. Stat. Phys.* **122**, 465 (2006).
- [16] A. Singer, Z. Schuss, and D. Holcman, *J. Stat. Phys.* **122**, 491 (2006).
- [17] S. Pillay, M. J. Ward, A. Peirce, and T. Kolokolnikov, *SIAM Multiscale Model. Simul.* **8**, 803 (2010).
- [18] A. F. Cheviakov, M. J. Ward, and R. Straube, *SIAM Multiscale Model. Simul.* **8**, 836 (2010).
- [19] A. F. Cheviakov, A. S. Reimer, and M. J. Ward, *Phys. Rev. E* **85**, 021131 (2012).
- [20] C. Caginalp and X. Chen, *Arch. Ration. Mech. Anal.* **203**, 329 (2012).
- [21] J.-F. Rupprecht, O. Bénichou, D. S. Grebenkov, and R. Voituriez, *J. Stat. Phys.* **158**, 192 (2015).
- [22] J. B. Garnett and D. E. Marshall, *Harmonic Measure* (Cambridge University Press, Cambridge, 2005).
- [23] C. W. Gardiner, *Handbook of Stochastic Methods for Physics, Chemistry and the Natural Sciences* (Springer, Berlin, 1985).
- [24] I. N. Sneddon, *Mixed Boundary Value Problems in Potential Theory* (Wiley, New York, 1966).
- [25] See Supplemental Material at <http://link.aps.org/supplemental/10.1103/PhysRevLett.117.260201> contains the derivation of the main formula (6), its numerical implementation and validation, some analytical results for disks and rectangles, the asymptotic behavior of the MFPT, iterative conformal map method for generation of irregular domains, and the discussion on the scaling of the MFPT with the area, which includes Ref. [26].
- [26] I. S. Gradshteyn and I. M. Ryzhik, *Table of Integrals, Series, and Products*, (Academic Press, New York, 1980).
- [27] M. Brady and C. Pozrikidis, *Proc. R. Soc. A* **442**, 571 (1993).
- [28] J. Koplik, S. Redner, and E. J. Hinch, *Phys. Rev. E* **50**, 4650 (1994).
- [29] J. Koplik, S. Redner, and E. J. Hinch, *Phys. Rev. Lett.* **74**, 82 (1995).
- [30] M. B. Hastings and L. S. Levitov, *Physica (Amsterdam)* **116D**, 244 (1998).
- [31] B. Davidovitch, H. G. E. Hentschel, Z. Olami, I. Procaccia, L. M. Sander, and E. Somfai, *Phys. Rev. E* **59**, 1368 (1999).
- [32] M. G. Blyth and C. Pozrikidis, *Int. J. Heat Mass Transfer* **46**, 1329 (2003).
- [33] M. Z. Bazant and D. Crowdy in the *Handbook of Materials Modeling*, edited by S. Yip *et al.* (Springer, New York, 2005), Vol. I, Art. 4.10.
- [34] X. Chen and A. Friedman, *SIAM J. Math. Anal.* **43**, 2542 (2011).
- [35] D. Holcman and Z. Schuss, *Rep. Prog. Phys.* **76**, 074601 (2013).
- [36] M. Z. Bazant, *Phys. Rev. Fluids* **1**, 024001 (2016).
- [37] A. Cherstvy, A. Chechkin, and R. Metzler, *New J. Phys.* **15**, 083039 (2013).
- [38] N. G. Makarov, *Proc. London Math. Soc.* **s3-51**, 369 (1985).
- [39] P. W. Jones and T. H. Wolff, *Acta Math.* **161**, 131 (1988).
- [40] B. Sapoval, *Phys. Rev. Lett.* **73**, 3314 (1994).
- [41] C. J. G. Evertsz, P. W. Jones, and B. Mandelbrot, *J. Phys. A* **24**, 1889 (1991).
- [42] M. E. Cates and T. A. Witten, *Phys. Rev. A* **35**, 1809 (1987).
- [43] P. Meakin, *Phys. Rev. A* **35**, 2234 (1987).
- [44] B. B. Mandelbrot and C. J. G. Evertsz, *Nature (London)* **348**, 143 (1990).
- [45] C. J. G. Evertsz and B. B. Mandelbrot, *J. Phys. A* **25**, 1781 (1992).
- [46] N. G. Makarov, *St. Petersburg Math. J.* **10**, 217 (1999).
- [47] B. Duplantier, *Phys. Rev. Lett.* **82**, 3940 (1999).
- [48] D. S. Grebenkov, A. A. Lebedev, M. Filoche, and B. Sapoval, *Phys. Rev. E* **71**, 056121 (2005).
- [49] E. Bettelheim, I. Rushkin, I. A. Gruzberg, and P. Wiegmann, *Phys. Rev. Lett.* **95**, 170602 (2005).
- [50] D. S. Grebenkov, *Phys. Rev. E* **91**, 052108 (2015).
- [51] D. S. Grebenkov, *Phys. Rev. Lett.* **95**, 200602 (2005).
- [52] P. Meakin, H. E. Stanley, A. Coniglio, and T. A. Witten, *Phys. Rev. A* **32**, 2364 (1985).
- [53] M. Filoche, D. S. Grebenkov, J. S. Andrade, and B. Sapoval, *Proc. Natl. Acad. Sci. U.S.A.* **105**, 7636 (2008).
- [54] J. S. Andrade, A. D. Araújo, M. Filoche, and B. Sapoval, *Phys. Rev. Lett.* **98**, 194101 (2007).
- [55] M. Felici, M. Filoche, and B. Sapoval, *J. Appl. Physiol.* **94**, 2010 (2003).
- [56] D. S. Grebenkov, M. Filoche, B. Sapoval, and M. Felici, *Phys. Rev. Lett.* **94**, 050602 (2005).
- [57] J. Gill, C. Salafia, D. S. Grebenkov, and D. Vvedensky, *J. Theor. Biol.* **291**, 33 (2011).
- [58] M. Mayo, S. Gheorghiu, and P. Pfeifer, *Phys. Rev. E* **85**, 011115 (2012).
- [59] R. Schinzinger and P. A. A. Laura, *Conformal Mapping: Methods and Applications* (Dover Publications, Mineola, 2003).
- [60] T. A. Driscoll and L. N. Trefethen, *Schwarz-Christoffel Mapping*, Cambridge Monographs on Applied and Computational Mathematics (Cambridge University Press, Cambridge, 2002).
- [61] L. Banjai and L. N. Trefethen, *SIAM J. Sci. Comput.* **25**, 1042 (2003).
- [62] D. E. Marshall and S. Rohde, *SIAM J. Numer. Anal.* **45**, 2577 (2007).